

# Building Blocks for a 10x10 Crossbar Switch based on GaAs/GaAlAs Channel Waveguide Array

Ray T. Chen  
Microelectronics Research Center  
Department of Electrical and Computer Engineering  
University of Texas, Austin  
Austin, TX 78759  
Tel: 512-471-7035

## ABSTRACT

In this paper, we proposed a all-optical crossbar switch based a successfully demonstrated a optically-activated modulator (OAM). This modulator was based on a GaAlAs/GaAs channel waveguide and waveguide array. A schematic of the demonstration is shown in Figure 1. A 5- $\mu\text{m}$  activation window was employed to input a  $\sim$  mW HeNe 632.8 nm light which, in turn, modulates the 1.3  $\mu\text{m}$  guided light. Modulation depths from 33% to 85% have been observed on the various devices tested. The size of the activation window is much smaller than for a linear electrooptic device ( $\sim$  mm to  $\sim$  cm) and a high power laser was not used in this demonstration. Consequently, this constitutes proof that a much more practical crossbar based on GaAs/GaAlAs channel waveguides can be built. The device architecture for the all-optical low-threshold 10x10 crossbar switch is shown in Fig.2 where semiconductor laser diode arrays with wavelength shorter than the band gap of GaAs semiconductor are employed to optically switch the propagation directions and thus receiving ports. Refractive index modulation as high as  $10^{-2}$  was achieved. Therefore, up to 100% on/off switching can be achieved within an activation length of 20  $\mu\text{m}$ .

## 1.0 INTRODUCTION

The first laser was built in the 1960's and within a decade laser beams spanning the range from infrared to ultraviolet were common. The availability of high power coherent sources led to the discovery of a number of new optical effects (second harmonic generation, linear and quadratic electrooptic effects, etc.) and thus to the development of a myriad of marvelous new devices. The technology needed to produce practical optical interconnection devices and systems is fast evolving.

The sophisticated use of crystals in devices such as second harmonic generators, electrooptics, acousto-optics, and magneto-optics has spurred a great deal of contemporary research in crystal optics. In the early 1970's, the concept of integrating different passive and active devices, such as lasers, waveguides, modulators, detectors, lenses, and prisms, in hybrid or monolithic forms was introduced. Integrated optoelectronics is a far-reaching attempt to apply thin film and integrated electronics technology to optical circuits and devices. By means of integrated optics, one has the potential to achieve higher speeds and more economical optical interconnection and data processing systems. Integrated optics can also provide a more convenient interface between optical and electronic systems.

One of the major building blocks of optoelectronic integrated circuits (OEIC) is the optical guided wave modulator. The realization of optical communication and computing with high parallelity, large modulation bandwidth and low propagation loss have made the optical wave an attractive information carrier.

To date, implementation of optical modulators is far from realization because of two basic factors. All-optical and electrooptic devices using either third order nonlinear optics ( $\chi^3$ ) or the second order nonlinear optics ( $\chi^2$ ) require high cost high power lasers [1-3] as the activation sources. In addition, due to the

difficulty of obtaining anything but a small index modulation, long interaction lengths [4-13] are mandatory, increasing device size and decreasing packing density.

Conclusions based on theoretical and experimental results are that (1) a device interaction length ( $5 \mu\text{m}$  in the demonstration [14,15]) shorter than that of MQW's is capable of generating a 33% to 85% modulation depth by using optical activation, (2) optical activation produces an index modulation two orders of magnitude larger than does the linear electrooptic effect ( $r_{41}$  in the case of GaAs), and (3) both all-optical and electrooptic modulators were proven to be feasible. Table 1 summarizes the experimentally confirmed features of the proposed crossbar Switch in comparison with existing devices.

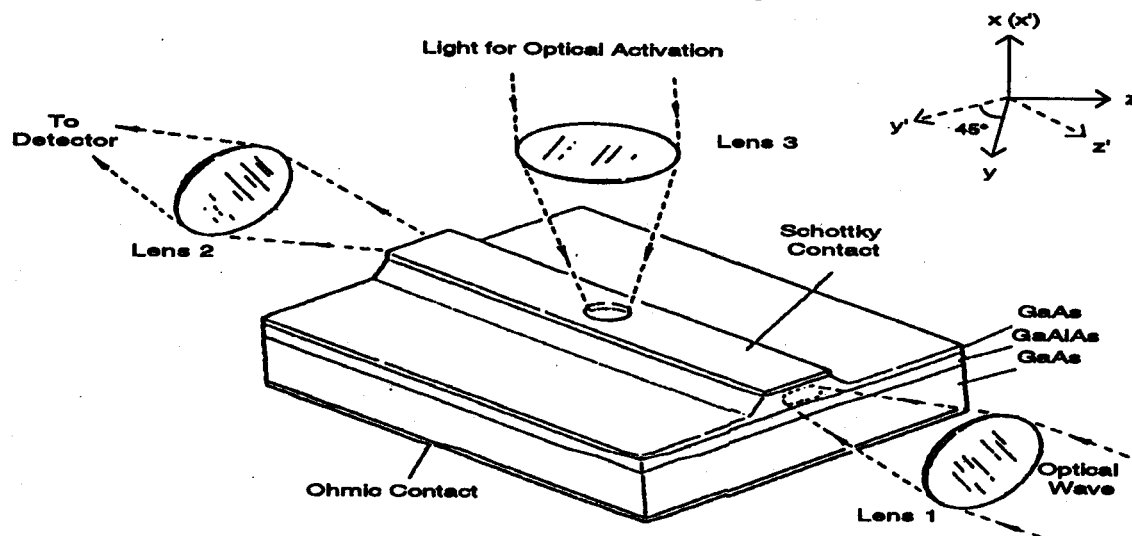


Figure 1  
Basic Structure of Optically Activated Modulator on GaAs Reported [15]

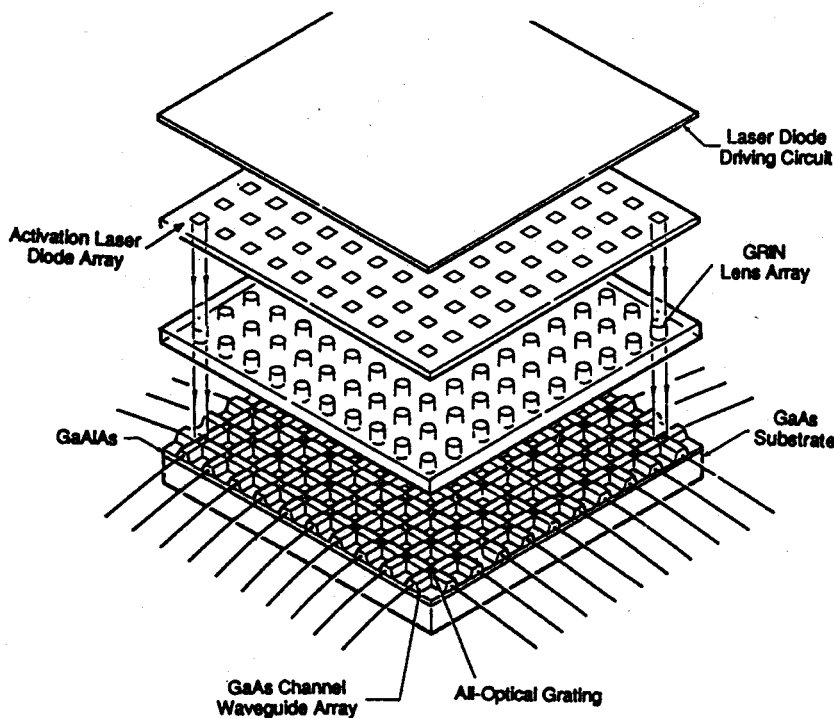


Figure 2  
Low Threshold 10x10 All-Optical Crossbar Switch Based on GaAs/GaAlAs Channel Waveguides

Table 1. Demonstrated Features of the GaAs Optically-Activated Crossbar in Comparison with Existing Active Devices

Technology Parameter	GaAs OAM	LiNbO <sub>3</sub> E-O Device	GaAs E-O Device	MQW	Plasmon Modulator	$\chi^{(3)}$ Nonlinear All-Optical Device
IR Optical Bandwidth	High	High	High	Very Low	Extremely Low	Low
Power Consumption	Low	High	High	Low	High	Very High
Status of Development	New Concept	Well Developed	Well Developed	Well Developed	Recently Developed	Recently Developed
Refractive Index Modulation	10 <sup>-2</sup>	10 <sup>-4</sup>	10 <sup>-4</sup>	10 <sup>-3</sup>	10 <sup>-4</sup>	10 <sup>-4</sup> - 10 <sup>-5</sup>
Extinction Ratio	High	High	High	High	High	High
Interaction Length	Short <sup>a</sup>	Long	Long	Short	Short	Short
Modulator Speed	High <sup>b</sup>	High	High	High	High <sup>c</sup>	High
Reliability	Very Good	Good	Good	Poor	Poor	Poor
Cost	Low	High	High	Very High <sup>d</sup>	High	Very High <sup>e</sup>
Practicality	Very Good	Good	Good	Poor	Poor	Poor
Coherence of Signal Carrier	Not Required <sup>f</sup>	Required	Required	Required	Required	Required

<sup>a</sup>5  $\mu\text{m}$  interaction length was demonstrated [14,15]

<sup>b</sup>Only limited by carrier lifetime which can be in the subpicosecond range.

<sup>c</sup>Theoretical prediction.

<sup>d</sup>Needs MBE machine to grow multilayer structure.

<sup>e</sup>Needs high power laser as the activation source.

<sup>f</sup>Both LEDs and LDs can be employed for the OAM working in the cutoff regime.

## 2.0 Principle of Operation and Device Structure

The throughput of data and signal processors are being pushed to ever increasing limits. The development of fast, more sophisticated integrated circuits and the use of parallel processing are largely responsible for this improvement. Due to the intrinsic material limitations of silicon, such as small electron and hole mobility (compared to GaAs), indirect band gap, and the inability to produce semi-insulating substrates, more and more research has been concentrated on other semiconductor materials which do not have these limitations. In order to provide high data rate communication, multi-giga hertz clock distribution and high packing density of interconnection channels, photons (bosons), instead of electrons (fermions), are taking over the role of signal carriers for many communication systems.

GaAs provides a direct band gap, high electron and hole mobilities, and semi-insulating substrate. The combination of these characteristics allows us to make high speed, monolithic, optoelectronic integrated circuits. In this paper, we propose, based on the reported results [14,15], to continue to develop a new two-dimensional GaAs-GaAlAs heterostructure channel waveguide modulator array. Optical waves of any light with wavelengths within the 0.9 to 1.5  $\mu\text{m}$  range can be used as the signal carrier. Optical photons from both coherent and incoherent light sources with  $h\nu > E_g$  (i.e., energy gap of GaAs waveguides) can be employed as the source for activating a vast number of free electrons and holes. The basic structure for the single-channel optically-activated modulator (OAM) on a GaAs-GaAlAs waveguide is shown in Figure 1. The small circular window area between the two electrode pads is designed to input the optical photons with

$h\nu > E_g$  to generate free electron and hole pairs. The optical wave representing the signal carrier can be coupled into the waveguide through end-firing or by a grating. A reverse bias can be added across the Schottky barrier to form a depletion region to accelerate the free carriers.

As shown in Figure 1, a Schottky contact is built on top of the channel waveguide. The reverse bias field added across the Schottky barrier is to increase photon generated electron-hole pairs (EHPs) within a diffusion length of the transition region in the semiconductor. The lack of free carriers within the space charge transition region can create a current due to the net generation of carriers by emission from recombination centers and valence band-to-conduction band transition.

It is clear from the discussion above that an optically activated modulator does not depend on the orientation of the GaAs crystal. The free-carrier induced index modulation reduces the effective index of the guided mode isotropically.

### 3.0 CHANNEL WAVEGUIDE DESIGN

From the experimental point of view, the key point of optimization of the single-mode channel waveguide at a given wavelength is the accuracy involved in determining the  $\Delta N$  value, i.e.,  $N_{\text{eff}} - N_s$  at the wavelength of interest. Theoretical work is needed first to obtain the proper waveguide parameters such as waveguide width and depth. The task is to precisely determine the effective index of the guided mode at the desired optical wavelengths under various waveguide dimensions and cladding layer indices. Among many different theoretical methods of determining the waveguide parameters, the two most frequently used are the effective index method [16] and Marcatili's method [17]. These approximation methods are quite accurate for the waveguide at well above the cutoff condition. For the waveguide near the cutoff, these two methods give a result with some discrepancy from that obtained by Goell's numerical method [18]. In the case of the channel waveguide involved in this work, the effective index method is not suitable unless the large difference in the index of refraction between the GaAs air interface has been taken care of. It has been found empirically that effective index method has better accuracy than the variational method if the effective index of the slab region is set equal to 1, which is the case for our waveguide, and the modes with effective index less than that of the substrate refractive index are disregarded. With this restriction in mind, the effective index method can also be used to determine the number of guided modes. The waveguide structures (Figures 1 and 2) we employed to perform optically activated modulation actually have trapezoid-shaped cross sections as shown in Figure 3. The variation of the angle  $\gamma$  from  $90^\circ$  is mainly due to the preferential etching by the chemical solution. As a result, the length of the base  $L_b$  is different from the length of the waveguide top  $L_t$ . If  $L_b = d$ , it follows that

$$L_t = d - 2 \cdot W \cdot \cot(\gamma), \quad (1)$$

where  $W$  is the waveguide thickness. The guided mode effective index and the number of guided modes lie between those of rectangular waveguides with width equal to  $L_t$  and  $L_b$ , respectively. The waveguides lying within these two boundary conditions are shown in Figures 3 (b) and (c). The parameters of these two waveguides serve as the upper and lower limits for the trapezoid-shaped waveguide. A theoretical calculation, based on Marcatili's method and the effective index method, is shown in Table 2. This result assures that the waveguide we used [15] is single mode.

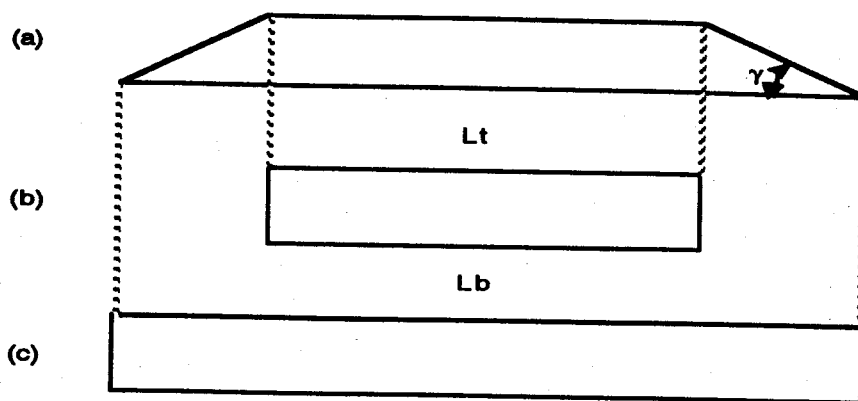


Figure 3  
 (a) Trapezoid-Shaped GaAs-GaAlAs Channel Waveguide.  
 (b) and (c) are Two Extreme Cases.

Realizing that all theoretical methods that predict channel waveguide effective indices are approximation methods to different degrees of accuracy, we use Marcatili's method to determine the upper boundary of waveguide cutoff dimensions at 1.3 and 1.55  $\mu\text{m}$  optical wavelengths with Al concentration equal to 5% and 7%. The results are displayed in Figures 4 and 5. Usually, Marcatili's method gives a shorter cutoff wavelength than Goell's numerical method.

One of the key elements for the realization of a GaAs-OAM-based crossbar switching system is the manipulation of the guided wave from one channel to the other channel (Figure 2) through optical illumination. As was reported in our previous publication[15], an index modulation as high as  $10^{-2}$  was achieved using a mW HeNe laser. Theoretically, the channel to channel switching efficiency can be expressed as

$$\eta = \sin^2 \left( \frac{\pi \Delta n \cdot d}{\lambda \cos \theta} \right) \quad (2)$$

Table 2. Number of Guided Modes of Different Waveguide Dimensions

Waveguide Parameter	GaAs-Ga <sub>0.93</sub> Al <sub>0.07</sub> As	
Operating Wavelength	1.32 $\mu\text{m}$	
Waveguide Thickness	0.9 $\mu\text{m}$	
Operating Width (mm)	Method	Number of Modes
3	Marcatili's	0
4	Marcatili's	0
5	Marcatili's	1
3	Effective Index	0
4	Effective Index	1
5	Effective Index	1

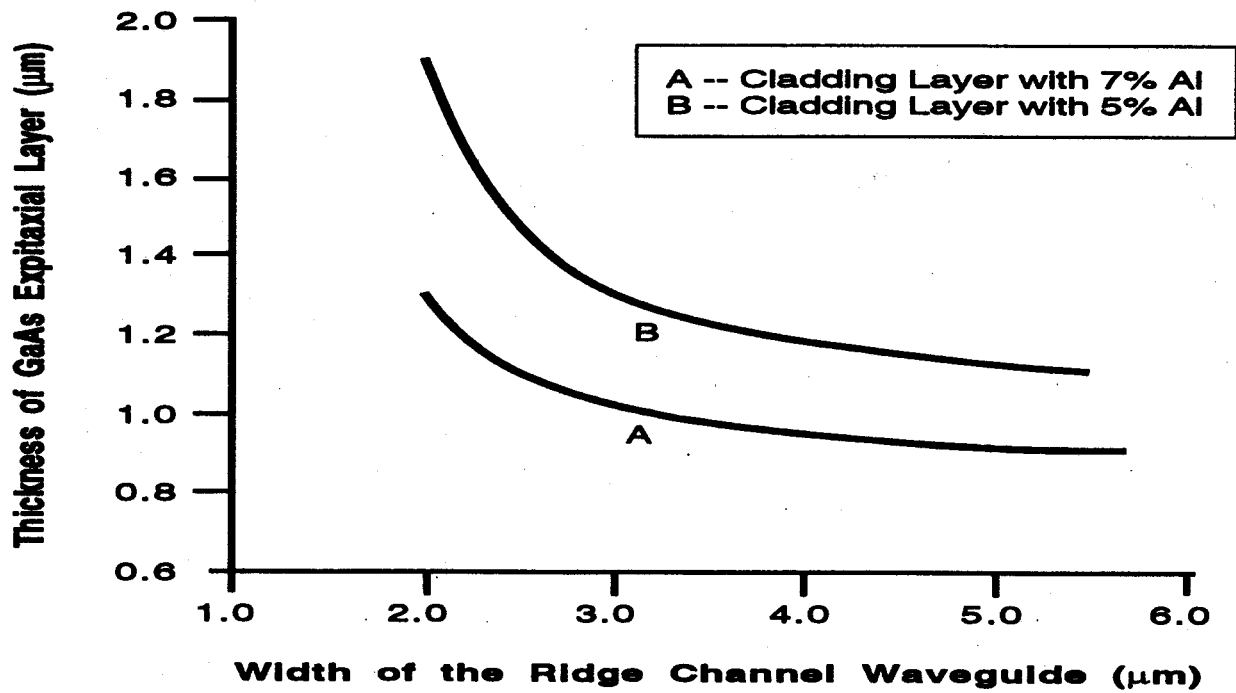


Figure 4  
The Calculated Results of Cutoff Dimension on GaAs-GaAlAs Heterostructure Ridge Channel Waveguide with Al = 5% and 7% at 1.3 μm Wavelength

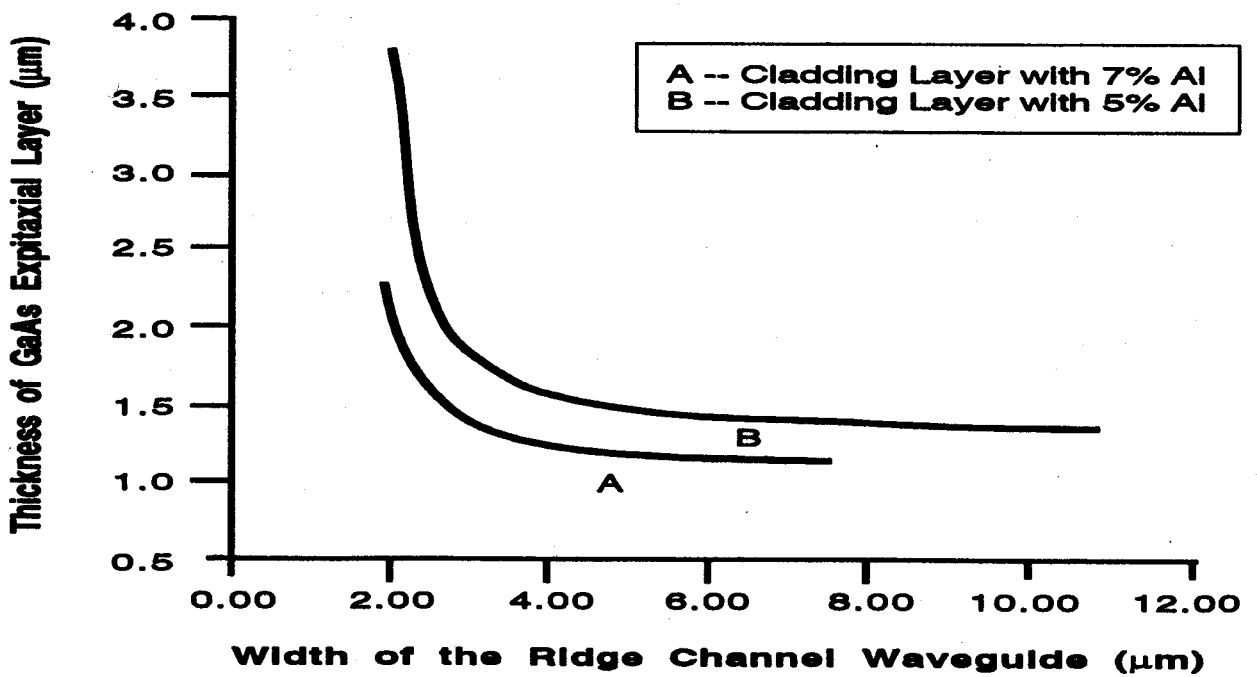


Figure 5  
The Calculated Results of Cutoff Dimension on GaAs-GaAlAs Heterostructure Ridge Channel Waveguide with Al = 5% and 7% at 1.55 μm Wavelength

where  $\lambda$  is the signal carrier wavelength,  $\Delta n$  is the optically induced index modulation,  $d$  is the interaction length and  $\theta$  is the channel-to-channel crossing angle,  $\pi/4$  in our current design (Figure 6). To produce 100% channel-to-channel switching, we have

$$d = \frac{\lambda \sin^{-1}(\sqrt{\eta})}{\sqrt{2} \cdot \pi \cdot \Delta n} \quad (3)$$

for  $\Delta n = 0.01$ , which is the magnitude of index modulation provided by optical activation, we have an interaction length of  $46 \mu\text{m}$ .

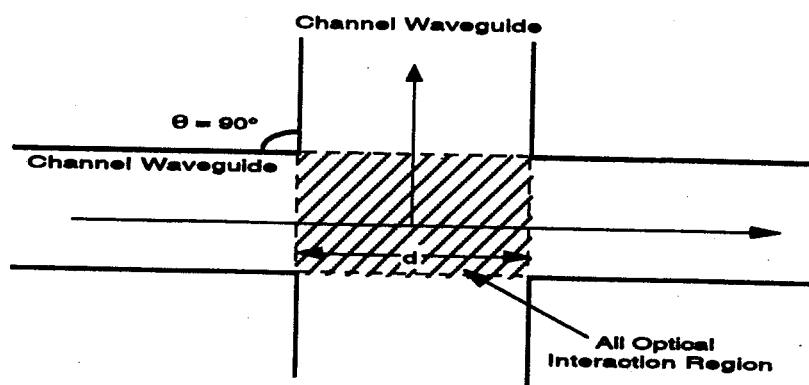


Figure 6  
Schematic of Channel-to-Channel Switching of the GaAs OAM

An interaction length of  $\sim 4 \text{ mm}$  is needed if  $\Delta n = 0.0001$ . Note that  $\Delta n \cong 10^{-4}$  is the magnitude of the index modulation for second and third order nonlinear effects due to the fact that the optimum  $d$  value is much larger than the optical waveguides of the signal carrier ( $1.3 \mu\text{m}$ ). It is also clear from the above numerical data that the architecture shown in Figure 1 is much easier for OAM which has  $\Delta n \cong 10^{-2}$ . A coupling horn structure shown in Figure 7 is needed to minimize the waveguide propagation loss. 1 to many fanout (Figure 2) can be easily realized by proportionally reducing the intensity of the laser diodes (activation sources) such that equal intensity may be achieved at all (up to 10) output channels.

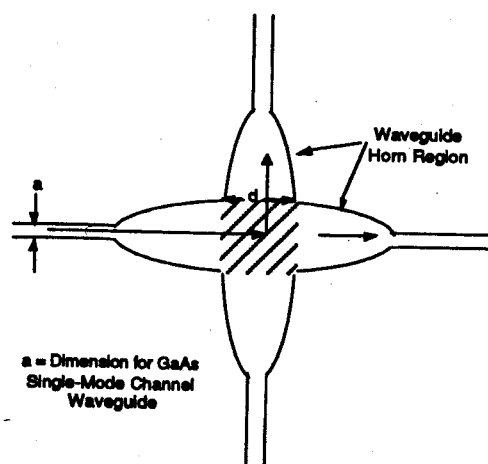


Figure 7  
Design of the Waveguide Horn to Incorporate Optimum Interaction Length  $d$  While Maintaining a Minimum Waveguide Propagation Loss

Horns are used in integrated optics to change the dimension of channel waveguides and to couple guided waves from a larger waveguide aperture to a smaller waveguide aperture and visa versa (Figure 9). Through the use of horns, waveguide devices such as all-optical gratings can be used in conjunction with channel waveguide arrays. To provide a low loss transition, the coupling horn must operate adiabatically. In other words, the lowest order local guided mode must propagate through the horn region without cumulative power transfer to higher order modes or substrate modes. The horn taper angle  $\theta$  (Figure 8) with a minimum negative effect of mode coupling [19] should be

$$\theta < (\lambda_g) / 2w \quad (4)$$

for all values of  $z$  (Figure 9) where  $\theta$  is the local half-angle of the horn at point  $z$ .  $\lambda_g$  is the wavelength of the lowest order local guided mode at point  $z$ , and  $w$  is the local full width of the horn at point  $z$ . A horn which satisfies our criteria for low loss operation can be obtained by setting [19]

$$\theta = \alpha \frac{\lambda_g}{2w} = \frac{1}{2} \frac{dw}{dz} \quad (5)$$

where  $\alpha$  is a constant less than unity. From Eq. (5), we can further derive

$$w = \sqrt{2\alpha\lambda_g z + w_D^2} \quad (6)$$

where  $w_D$  is the horn width at  $z = 0$ . A parabolic horn designed with  $\alpha = 1$  has been experimentally investigated and has been shown to be low loss.

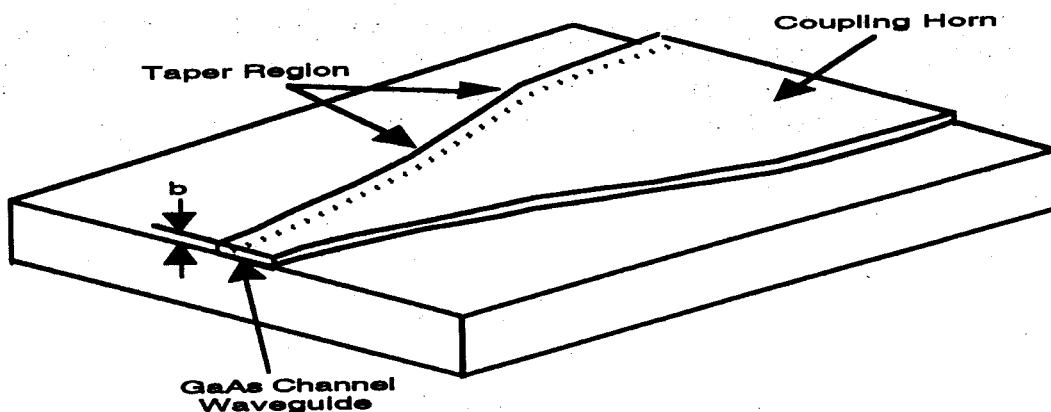


Figure 8  
The Horn Structure for Waveguide Coupling

#### 4.0 SELFOC Micro Lens Array

To collimate and focus the visible semiconductor laser lights (Figure 2) onto the active areas, i.e., all-optical gratings, of the GaAs channel waveguide arrays, a SELFOC lens array (SLA) is needed. The SELFOC lens is a unique, cylindrical lens having a parabolic refractive index distribution which is highest on its optical axis and decreases toward the periphery as the square of the radial distance from the optical axis. The refractive index at any point  $r$  (Figure 10) from the optical axis is given by



$$N_r = N_0 \left( 1 - \frac{A}{2} \cdot r^2 \right) \quad (7)$$

where  $N_r$  is the refractive index at any point  $r$ ,  $N_0$  is the refractive index on the optical axis,  $A$  is the quadratic gradient constant at the wavelength of use ( $\text{mm}^{-2}$ ),  $r$  is the radial distance between any point on the lens and the optical axis, and finally  $i$  is the incident emitting angle. A meridional ray entering the SELFOC at  $r_1$  and  $i_1$  will exit at  $r_2$  and  $i_2$  as shown in Figure 10. Thus, the ray matrix of a SELFOC lens can be derived from the equation:

$$\begin{pmatrix} r_2 \\ i_2 \end{pmatrix} = \begin{pmatrix} \cos(\sqrt{A} Z) & \sin(\sqrt{A} Z / N_0 \sqrt{A}) \\ -N_0 \sqrt{A} \sin(\sqrt{A} Z) & \cos(\sqrt{A} Z) \end{pmatrix} \begin{pmatrix} r_1 \\ i_1 \end{pmatrix} \quad (8)$$

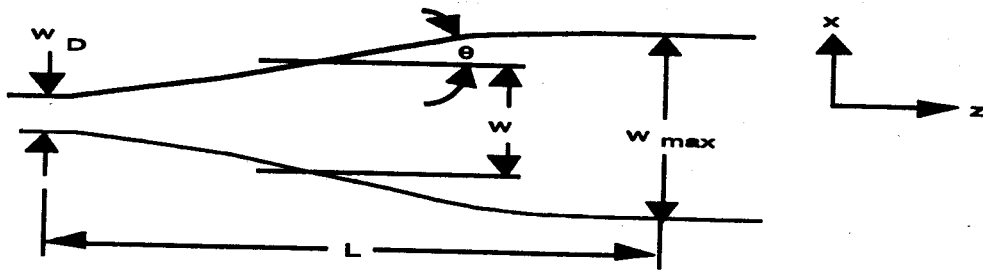


Figure 9  
Top View of the Horn

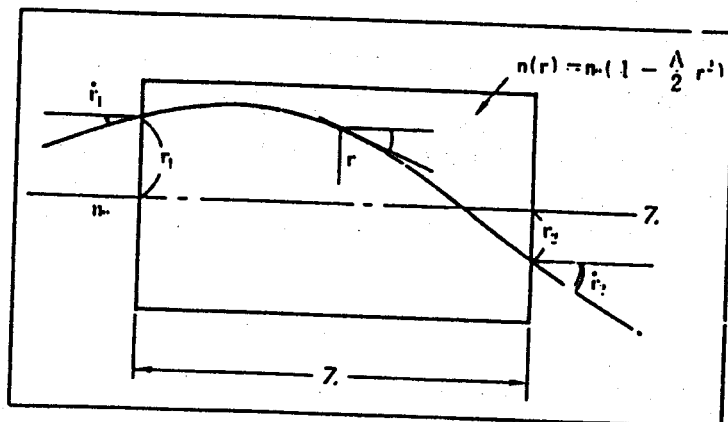


Figure 10  
Beam Propagation Within the SELFOC Lens

The length of the SELFOC micro lens array can be adjusted to exactly 1/4 pitch at the activation wavelength such that a focused beam can be achieved from the output end face. The length corresponding to quarter pitch is

$$L = \frac{1}{4} \cdot \frac{2\pi}{\sqrt{A}} \text{ (mm)} \quad (9)$$

which can be determined experimentally by measuring the value of A.

## 5.0 Carrier Lifetimes in GaAs

The limiting factor of the optically activated modulator (OAM) is the carrier lifetime which determines the switching speed of the device. For intrinsic GaAs, a carrier lifetime on the order of ~ 10 nsec is routinely reported. A carrier lifetime as short as  $0.6 \pm 0.2$  psec was achieved on (100) semi-insulating (SI) liquid-encapsulated Czochralski (LEC) GaAs using H<sup>+</sup> ion implantation [20]. The switching time of the device can be estimated by

$$\Delta T = \frac{2\pi}{\Delta\tau} \quad (10)$$

where  $\Delta\tau$  is the mean carrier lifetime of the device.

## 6.0 CONCLUSIONS

In this paper, we proposed a all-optical crossbar switch based a successfully demonstrated a optically-activated modulator (OAM). This modulator was based on a GaAlAs/GaAs channel waveguide and waveguide array. A schematic of the demonstration is shown in Figure 1. A 5- $\mu\text{m}$  activation window was employed to input a ~ mW HeNe 632.8 nm light which, in turn, modulates the 1.3  $\mu\text{m}$  guided light. Modulation depths from 33% to 85% have been observed on the various devices tested. The size of the activation window is much smaller than for a linear electrooptic device (~ mm to ~ cm) and a high power laser was not used in this demonstration. Consequently, this constitutes proof that a much more practical crossbar based on GaAs/GaAlAs channel waveguides can be built. The device architecture for the all-optical low-threshold 10x10 crossbar switch is shown in Fig.2 where semiconductor laser diode arrays with wavelength shorter than the band gap of GaAs semiconductor are employed to optically switch the propagation directions and thus receiving ports. Refractive index modulation as high as  $10^{-2}$  was achieved. Therefore, up to 100% on/off switching can be achieved within an activation length of 20  $\mu\text{m}$ .

## 7.0 REFERENCES

1. S. M. Sze, *Physics of Semiconductor Devices*, 2nd ed., p. 851 (John Wiley & Sons, 1981).
2. See, for example, D. H. Auston, *Appl. Phys. Lett.*, **26**, 101 (1975); J. A. Buck, K. K. Li, and J. R. Whinnery, *J. of Applied Physics*, **51**, 769 (1980); P. Cheung, et al., *IEEE Trans Microwave Theory and Tech.*, **38**, 586 (1990); and C. H. Lee, *IEEE Trans Microwave Theory and Tech.*, **38**, 596 (1990).
3. M. B. Johnson and T. C. McGill, *Appl. Phys. Lett.*, **54**, 2424 (1989).
4. M. Papuchon, et al., "Electrically Switched Optical Directional Coupler: Cobra," *Appl. Phys. Lett.*, **27**, 289 (1975).

5. R. C. Alferness, R. V. Schmidt, and E. H. Toner, "Characterization of Ti-Diffused LiNbO<sub>3</sub> Optical Directional Couplers, *Appl. Opt.*, **18**, 4012 (1979).
6. W. E. Marin, "A New Waveguide Switch/Modulator for Integrated Optics," *Appl. Phys. Lett.*, **32**, 562 (1975).
7. V. Ramaswamy, M. D. Divino, and R. D. Standley, "Balanced Bridge Modulator Switching Using Ti-Diffused LiNbO<sub>3</sub> Strip Waveguides," *Appl. Phys. Lett.*, **32**, 644-646 (1978).
8. C. L. Chang and C. S. Tsai, "Electrooptic Analog-to-Digital Converter Using Channel Waveguide Fabry-Perot Modulator Array," *Appl. Phys. Lett.*, **43**, 22 (1983).
9. S. Y. Wang, S. H. Lin, and M. Huong, "GaAs Traveling-Wave Polarization Electro-Optic Waveguide Modulator with Bandwidth in Excess of 20 GHz at 1.3  $\mu$ m," *Appl. Phys. Lett.*, **51**, 83 (1987).
10. R. T. Chen, "E-O Depolarization Switch on Y-Cut LiNbO<sub>3</sub> PE Channel Waveguides," *Appl. Phys. Lett.*, **54**, 2628 (1989).
11. R. Chen and C. S. Tsai, "Thermally Annealed Single-Mode Proton-Exchanged Channel Waveguide Cut Off Modulator," *Opt. Lett.*, **11**, 546 (1986).
12. R. Chen, "Thermally Annealed Mode Annihilation Switching Array on Proton Exchanged LiNbO<sub>3</sub> Channel Waveguides," SPIE, San Diego, CA, 1989.
13. R. Chen, et al., "GaAs-GaAlAs Heterostructure Single-Mode Channel Waveguide Cutoff Modulator and Modulator Array," *IEEE J. of Quantum Electron.*, **QE-23**, 2205 (1987).
14. Ray T. Chen, "Single-Mode Optically-Activated Phase Modulator On GaAs/GaAlAs Compound Semiconductor Channel Waveguides," 1992 SPIE OE/FIBER Symposium, Vol. 1794-12.
15. Ray T. Chen, "GaAs/GaAlAs Electrooptic and All-optical Switching Array and Its Applications," To Appear in the *Journal of Applied Physics*.
16. B. Hocker and W. K. Burns, "Mode Dispersion in Diffused Channel Waveguides by Effective Index Method," *Appl. Opt.*, **16**, 113 (1977).
17. E. A. J. Marcatili, "Dielectric Rectangular Waveguide and Directional Coupler for Integrated Optics," *Bell Sys. Tech. J.*, **48**, 2071 (1969).
18. J. E. Goell, "Loss Mechanisms in Dielectric Waveguide," *Introduction to Integrated Optics*, Chapter 5.
19. W. K. Brown et al., "Optical Waveguide Parabolic Coupling Horns," *Appl. Phys. Lett.*, **30**, 28 (1977).
20. See, for example,  
 D. H. Auston, *Appl. Phys. Lett.*, **26**, 101 (1975).  
 J. A. Buck, K. K. Li, and J. R. Whinnery, *J. Appl. Phys.*, **51**, 769 (1980).  
 P. Cheung et al., *IEEE Trans. Microwave Theory and Tech.*, **38**, 586 (1990).  
 C. H. Lee, *IEEE Trans. Microwave Theory and Tech.*, **38**, 596 (1990).